

## INVESTIGATION OF SURFACE ACOUSTIC WAVE MOTOR'S MOTION RESOLUTION DETERMINANT

T. Shigematsu <sup>\*\*</sup>, M. K. Kurosawa <sup>\*</sup> and K. Asai <sup>\*\*</sup>

<sup>\*</sup>Department of Advanced Applied Electronics, Tokyo Institute of Technology, Yokohama, Japan.

<sup>\*\*</sup>Advanced Technology Research Laboratories, Matsushita Electric Industrial Co., Ltd., Kyoto, Japan.

<sup>#</sup> tucker@ae.titech.ac.jp

### Abstract

A surface acoustic wave (SAW) motor exhibits sub-nanometer motion resolution, over centimeter-level long stroke. The determinant of the motion resolution was experimentally investigated. The experimental results indicated that amplitude of Rayleigh wave, which is utilized for friction drive, determined the motion resolution. The stepping drives by 20-nm amplitude Rayleigh wave limited the resolution to 1 nm. However, by using 9-nm amplitude Rayleigh wave, 0.5 nm stepping drive was achieved. The smaller amplitude achieved the higher resolution stepping motion.

### Introduction

Since ultrasonic motors (USMs) have high-resolution, high-holding torque/force and ability of direct drive characteristics, they are recently regarded as suitable actuators for precision equipments or reasonable alternatives to electromagnetic motors in the marketplace. A motion resolution of an USM seems to be dependent on amplitude of a stator vibration. That is recognized as the reason why a SAW motor exhibits higher resolution motion, ranging down to sub-nanometer, than conventional USMs do [1][2]. However, a motion resolution determinant or relations between the motion resolution and driving parameters, *e.g.* vibration amplitude or a pre-load, of an USM has not yet discussed. We discuss the motion resolution's determinant and relations to the driving parameters of the SAW motor in this paper.

### Principle

A schematic view of a SAW motor is illustrated in Fig. 1. A SAW device (stator) is made of  $128^\circ$  y-rotated x-propagating  $\text{LiNbO}_3$  substrate. Both end of the stator, interdigital transducers (IDTs) are located. RF electrical power (9.6 MHz) is transduced to Rayleigh wave at the IDT. The propagating Rayleigh wave energy is transferred to a mechanical slider motion through frictional force [3].

Surface particles of the stator move in elliptical motion when the Rayleigh wave propagates. The rotating

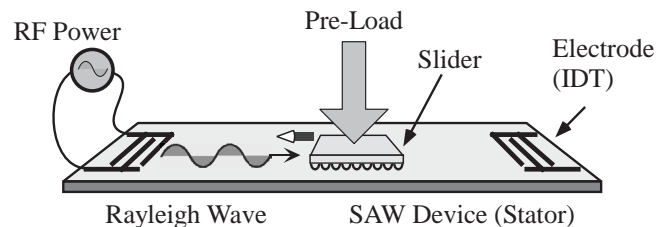


Figure 1: Schema of a surface acoustic wave motor.

surface particles contact the slider surface at its making wave crests. The particle motion, then, drives the slider through frictional force. The Rayleigh wave amplitude on the stator is several tens of nanometers at most. To control the contact condition in order to utilize the small amplitude vibration and to obtain output power efficiently, a surface microfabricated silicon substrate element has been used as the slider. Many cylindrical projections were fabricated on the surface as depicted in Fig. 2. A diameter and/or a pitch of the projections extremely change a motor performance [4]. Pre-load to the slider enlarges the output force due to the enlarged frictional force.

### Experimental Setup

An experimental setup is shown in Fig. 3. A stator was fixed on a glass substrate, which was connected to a base. A linear guide rail was fixed to a steel block that could only vertically move in the figure. The stator and the rail were installed in parallel. A washer was glued onto a linear guide stage. A steel hemisphere, which was glued to the slider, was put in the washer. The hemisphere-washer connection yielded a self-alignment structure to maintain the slider and stator surfaces' parallel contact condition.

The stator was  $60 \times 15 \times 1 \text{ mm}^3$ . At each end of the stator, IDTs were fabricated. The dimensions of the IDT were 0.4 mm in pitch, 0.1 mm in electrode strip width and 9 mm in aperture. The IDT was composed of 20 strip electrode pairs and the resonance frequency for Rayleigh wave generation was 9.6 MHz. A silicon slider was  $4 \times 4 \times 0.6 \text{ mm}^3$ .

The stroke of the slider motion was 25 mm. A laser beam of the laser Doppler interferometer was incident

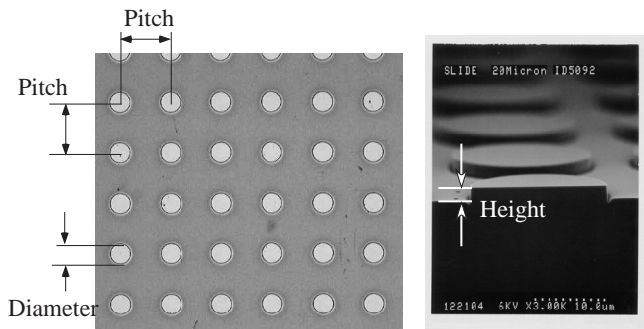
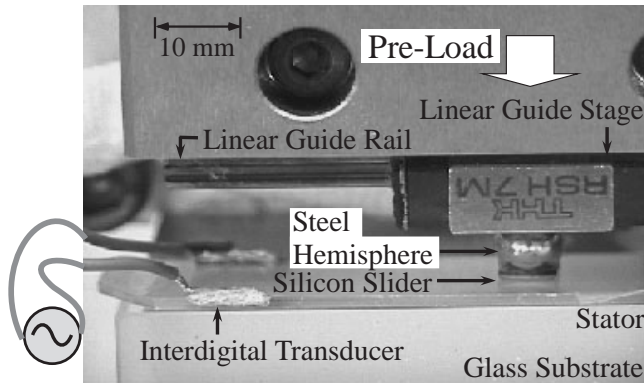


Figure 2: Micro cylindrical projections, which were fabricated on a slider surface.



RF Power (9.6 MHz)

Figure 3: Experimental Setup.

on the steel hemisphere to measure the silicon slider's motion. The pre-load was given by a coil spring, thus, the pre-load easily adjusted. Burst driving voltage was applied to the IDT every 0.2 ms to drive the motor in a stepping motion.

### Minimum Stepping Motion

Driving voltage, pre-load and a number of driving waves were the parameters to change the step size of a stepping motion [2]. The number of driving waves was the easiest parameter to control the stepping motion, while the other two parameters were kept constant. Thus, under each constant driving voltage and pre-load condition, we sought out a minimum stepping motion by means of driving waves' decrement. Decreasing the number of driving waves one by one easily exhibited a minimum stepping motion under each condition, in a manner similar to the stepping motions indicated in Figs. 4 and 5.

### Definition

As shown in Fig. 4, under the conditions of 10 N pre-load and 60 V<sub>peak</sub> driving voltage, which yielded 13-nm amplitude Rayleigh wave, 23 cycles of driving waves produced approximately 0.5 nm stepping motion. The drive by 22 cycles of waves, which only one cycle smaller than 23 waves, did not result a stepping motion as shown

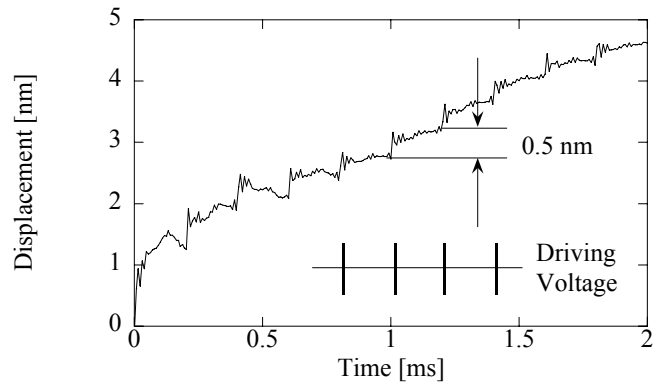


Figure 4: A minimum stepping motion of the slider; the driving voltage was 60 V<sub>peak</sub>, the pre-load was 10 N, the driving waves were 23 cycles and the burst period was 0.2 ms. The traced data was the average of 30 motions. Approximately 0.5 nm stepping motion.

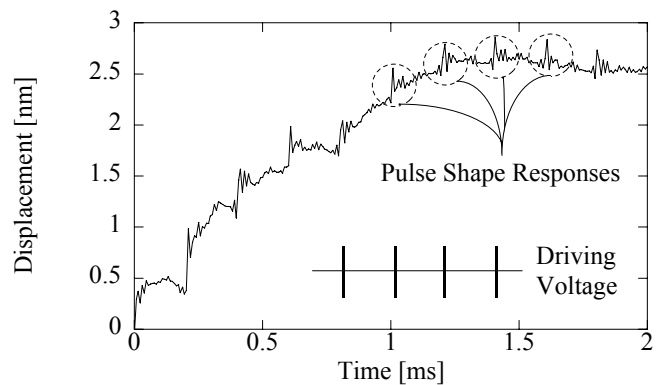


Figure 5: A motion, underrunning a minimum friction drive, of the slider; the driving voltage was 60 V<sub>peak</sub>, the pre-load was 10 N, the driving waves were 22 cycles, which was 1 wave number smaller than that of Fig. 4. The burst period was 0.2 ms. The indicated data was the average of 30 motions.

in Fig. 5. Pulse shape responses were yielded when the Rayleigh wave was underneath the slider, however a step motion was not performed. There was a boundary, whether or not the slider could be driven, in decreasing the number of driving waves. We determined the stepping motion indicated in Fig. 4 as the minimum stepping motion under this condition.

### Pulse Shape Response

The movable part of the experimental set up behaved as 2-degree-of-freedom vibration system in nanometer scale [5][6], as illustrated in Fig. 6. Elastic deformations, which arose from the friction drive, in the movable part caused this vibration system. Since the spring constant of  $k_2$  in the figure, namely elastic connection between the steel hemisphere and the washer, was more than 10 times smaller than that of  $k_1$ [6], it was recognized that the spring  $k_2$  did not prevent the slider motion. In addition, it was regarded that the friction between the linear guide

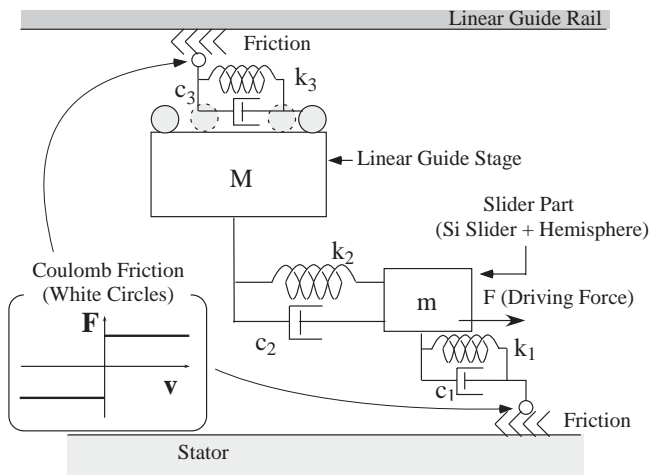


Figure 6: Mechanical model of the movable part.

stage and the linear guide rail, and the elastic components  $k_3$  and  $c_3$  were negligible. Therefore, it is possible to say that the pulse shape responses were happened at the slider-stator contact boundary. A minimum limit of a stepping motion was, thus, recognized as a matter of the friction drive principle.

### Step Size Determinant

The minimum stepping motions under various pre-load and driving voltage--practically vibration amplitude of Rayleigh wave--conditions were sought out in the way that discussed in *Minimum Stepping Motion* section. Seven kinds of sliders, which were different in projections' parameters, were tested, since the difference of the slider figuration highly differed the motor performance [4]. To evaluate the minimum stepping motions, the displacement value "friction driven displacement" is introduced. The displacement that occurred while the Rayleigh wave was underneath the slider slightly differed from the step size. The mechanical structure of the movable part caused the difference [5]. The displacement while the Rayleigh wave was under the slider indirectly indicated friction drive property [2]. Thus, we named it "friction driven displacement" and used for the evaluation of the friction drive property.

### Pre-load

A friction driven displacement and a step size of a minimum stepping motion under each pre-load condition were measured, while the driving voltage was  $60 V_{peak}$ ; Rayleigh wave amplitude was 13 nm. The experimented slider had 40  $\mu m$  pitch arrayed 20  $\mu m$  diameter and 2  $\mu m$  height projections. The friction driven displacements or the step sizes were distributed randomly ranging around 1 nm, as indicated in Fig. 7. However, as shown in Fig. 8, the ratio of a step size to a friction driven

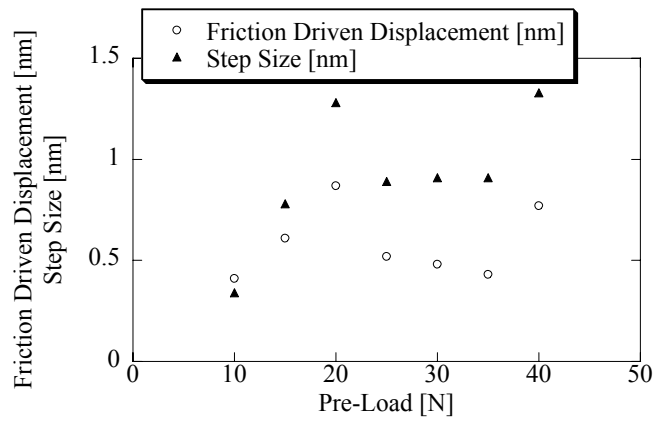


Figure 7: The friction driven displacements and the step sizes of the minimum stepping motions in relation to the pre-load; the driving voltage was  $60 V_{peak}$ .

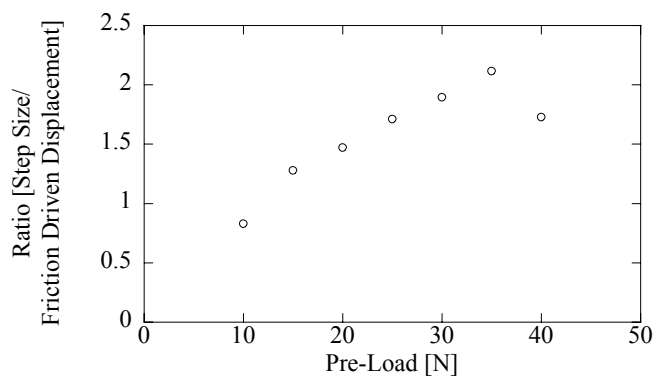


Figure 8: The ratio of step size to friction driven displacement of the minimum stepping motions in relation to the pre-load; the driving voltage was  $60 V_{peak}$ .

displacement increased in keeping with the pre-load. Since the increase of pre-load stiffened the hemisphere-washer connection, the silicon slider part was easily dragged forward by the inertia of the linear guide stage. Hence, it can be said that the pre-load did not affect the minimum friction driven displacement however the increase of the pre-load enlarged the step size.

### Rayleigh wave amplitude

The minimum friction driven displacements of the minimum stepping motions in relations to the Rayleigh wave amplitude were investigated. The pre-load or the driving voltage was changed from 5 N to 20 N or from  $40 V_{peak}$  to  $80 V_{peak}$ ; the steady state Rayleigh wave amplitude was 9 nm to 18 nm. The slider that had 40  $\mu m$  pitch arrayed 20  $\mu m$  diameter and 2  $\mu m$  height projections was used. The results were plotted in Fig. 9 in terms of the pre-load. The result indicated in Fig. 9 reassured the discussion in *Pre-load* subsection that the pre-load did not determine the minimum friction driven displacement. It seems that the smaller Rayleigh wave amplitude yielded the smaller minimum friction driven

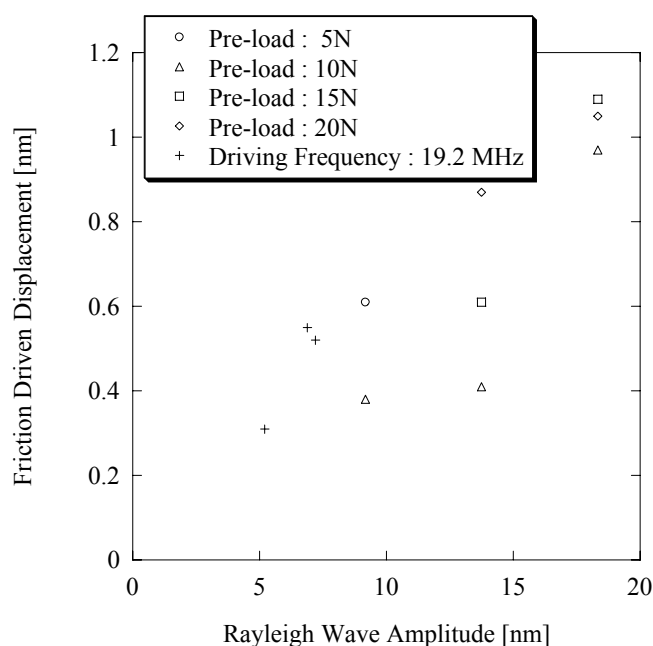


Figure 9: The minimum friction driven displacements in relation to the Rayleigh wave amplitude; pre-load was from 5 N to 20 N, the driving frequency was 9.6 MHz, except the term 19.2 MHz driving frequency.

displacement. The drive by the 9-nm amplitude Rayleigh wave brought about minimum 0.4 nm friction driven displacement.

To investigate further the relationship between Rayleigh wave amplitude and friction driven displacement, the minimum stepping motion seeking by means of the twice driving frequency, 19.2 MHz, stator was examined. The twice frequency vibration has the twice vibration velocity if the amplitude is same. The experimental results are indicated in Fig. 9. The 19.2-MHz stator enabled the drives by means of smaller amplitude: the plotted results were on an extension of the other results' dispersion.

#### Slider Surface Topology

Projections' parameter of a slider, namely height, diameter and pitch, changes the motor performance [4]. The characteristics of minimum friction driven displacements of seven different projections' parameter sliders were examined. The projections' parameters were varied within 0.5  $\mu\text{m}$  to 2  $\mu\text{m}$  of height, 5  $\mu\text{m}$  to 20  $\mu\text{m}$  of diameter, and 10  $\mu\text{m}$  to 40  $\mu\text{m}$  of pitch. The results are indicated in Fig. 10 as in terms of the slider parameters. In Fig. 10, the plotted data in Fig. 9 are also indicated. Almost all the plots existed within a dispersion of the results indicated in Fig. 9. The slider surface topology changes the output force and the no-load speed of the motor, however did not seem to have an influence on the minimum friction driven displacement.

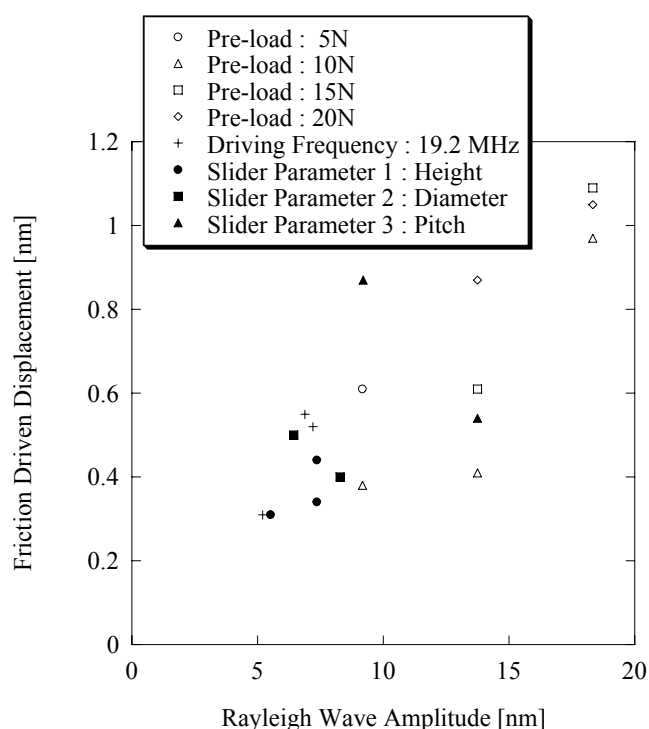


Figure 10: The minimum friction driven displacements in relation to the Rayleigh wave amplitude; pre-load parameter was from 5 N to 20 N, seven different projections' parameter sliders were used. The slider parameters were height, diameter and pitch.

#### Conclusion

The experimental results using seven kinds of sliders, or of the various pre-load conditions did not show obvious difference of the minimum friction driven displacement. Only the Rayleigh wave amplitude determined the minimum friction driven displacement. On one hand, the increase of pre-load enlarged the step size because of the mechanics.

#### Acknowledgement

This work was supported by a Grant-in-Aid for the Development of Innovative Technology of the Ministry of Education, Culture, Science and Technology of Japan.

#### References

- [1] M. Kurosawa et al., "Ultrasonic Linear Motor Using Surface Acoustic Waves," *Tran. UFFC*, Vol. 43, pp. 901-906, 1996.
- [2] T. Shigematsu et al., "Nanometer Stepping Drives of Surface Acoustic Wave Motor," *Tran. UFFC*, Vol. 50, pp. 376-385, 2003.
- [3] K. Asai et al., "Evaluation of the driving performance of a surface acoustic wave linear motor," in *Proc. IEEE Ultrason. Symp.*, pp. 675-679, 2000.
- [4] M. K. Kurosawa et al., "Optimization of Slider Contact Face Geometry for Surface Acoustic Wave Motor," in *Proc. IEEE MEMS*, pp. 252-255, 2001.
- [5] T. Shigematsu et al., "Experimental Study of Surface Acoustic Wave Motor Stepping Motion," in *Proc. THE 20th SENSOR SYMPOSIUM*, pp. 51-56, 2003.
- [6] T. Shigematsu et al., "Stepping Motion Analysis of Surface Acoustic Wave Motor toward Nanometer Resolution Positioning System," in *Proc. IEEE Ultrason., Symp.*, pp. 635-638, 2002.